Supporting Information

Responses of the proteome and metabolome in livers of zebrafish exposed chronically to environmentally relevant concentrations of microcystin-LR

Liang Chen[†,‡,#], Yufei Hu[†,‡,#], Jun He[†], Jun Chen[†,*], John P. Giesy[§,∥,⊥], Ping Xie[†,*]

† Donghu Experimental Station of Lake Ecosystems, State Key Laboratory of Freshwater Ecology and Biotechnology, Institute of Hydrobiology, Chinese Academy of Sciences, Wuhan, 430072, China

‡ University of Chinese Academy of Sciences, Beijing, 100049, China

§ Department of Veterinary Biomedical Sciences and Toxicology Centre, University of Saskatchewan, Saskatoon, Saskatchewan S7N 5B3, Canada

∥ School of Biological Sciences, University of Hong Kong, Hong Kong SAR, China

⊥ State Key Laboratory of Pollution Control and Resource Reuse, School of the Environment, Nanjing University, Nanjing, 210089, China

 # These authors contributed equally to this work.

* **Authors for correspondence:** Jun Chen (Dr.), E-mail: chenjun@ihb.ac.cn, Ping Xie (Dr.), E-mail: xieping@ihb.ac.cn, Tel./Fax: +86-27-68780622, Institute of Hydrobiology, Chinese Academy of Sciences, No. 7 Donghu South Road, Wuhan, 430072, China

17 pages, 4 figures, 3 tables

Summary

iTRAQ-based quantitative proteomic analysis

Extraction of Proteins

Samples of liver were ground while frozen in liquid nitrogen, then powdered cells were transferred to 5 mL centrifuge tubes and sonicated three times on ice using a high intensity ultrasonic processor (Scientz) in lysis buffer (8 M urea, 1% Triton-100, 10 mM dithiothreitol (DTT, Sigma) and 0.1% Protease Inhibitor CocktailIV). The remaining debris was removed by centrifugation at 20,000g at 4 °C for 10 min. Finally, the protein was precipitated with cold 15% trichloroacetic acid (TCA) for 2 h at -20 °C. After centrifugation at 4 °C for 10 min, the supernatant was discarded. The remaining precipitate was washed with cold acetone for three times. The protein was redissolved in buffer (8 M urea, 100 mM TEAB, pH 8.0) and quantified by use of the 2-D Quant kit (GE Healthcare, Pittsburgh, PA) according to instructions provided by the manufacturer.

Digestion by Trypsin

For digestion, protein was reduced with 10 mM DTT for 1 h at 37 °C and alkylated with 20 mM iodoacetamide (IAA, Sigma) for 45 min at room temperature in darkness. For digestion with trypsin protein was diluted by adding 100 mM TEAB to a concentration of urea less than 2 M. Sequencing Grade Modified Trypsin (Promega) was then added at 1:50 trypsin-to-protein mass ratio for the first digestion overnight and 1:100 trypsin-to-protein mass ratio for a second digestion for 4 h. Approximately 100 μg protein for each sample was digested with trypsin for the following experiments.

iTRAQ Labeling

After digestion of proteins by trypsin, peptides were desalted by use of a Strata X C18 SPE column (Phenomenex) and vacuum-dried. Peptides were reconstituted in 0.5 M TEAB and processed according to the manufacturer’s protocol for 8-plex iTRAQ kit (AB Sciex, Foster City, CA). Briefly, one unit of iTRAQ reagent (defined as the amount of reagent required to label 50 μg of peptide) was thawed and reconstituted in

24 μl acetonitrile (ACN, Fisher Chemical). Mixtures of peptides were then incubated for 2 h at room temperature and pooled, desalted and dried by vacuum centrifugation.

Fractionation by HPLC

Samples were then fractionated by use of high pH, reverse-phase high-performance liquid chromatography (HPLC) using Agilent 300Extend C18 column (5 μm particles, 4.6 mm ID, 250 mm length, Santa Clara, CA). Briefly, peptides were first separated with a gradient of 2% to 60% acetonitrile in 10 mM ammonium bicarbonate pH 10 over 80 min into 80 fractions, Peptides were then combined into 18 fractions and dried by vacuum centrifuging.

LC-MS/MS Analysis

Peptides were dissolved in 0.1% formic acid (FA, Fluka), directly loaded onto a reversed-phase pre-column (Acclaim PepMap 100, Thermo Scientific). Separation of peptides was performed using a reversed-phase analytical column (Acclaim PepMap RSLC, Thermo Scientific). The gradient was comprised of an increase from 6% to 22% solvent B (0.1% FA in 98% ACN) over 26 min, 22% to 35% in 8 min and climbing to 80% in 3 min then holding at 80% for the last 3 min, all at a constant flow rate of 300 nl/min on an EASY-nLC 1000 UPLC system, The resulting peptides were analyzed by Q Exactive^{TM} Plus hybrid quadrupole-Orbitrap mass spectrometer (ThermoFisher Scientific, Waltham, MA).

Peptides were subjected to NSI source followed by tandem mass spectrometry (MS/MS) in Q Exactive^{TM} Plus (Thermo) coupled online to the ultra performance liquid chromatography (UPLC). Intact peptides were detected in the Orbitrap at a resolution of 70,000. Peptides were selected for MS/MS using NCE setting as 30; ion fragments were detected in the Orbitrap at a resolution of 17,500. A data-dependent procedure that alternated between one MS scan followed by 20 MS/MS scans was applied for the top 20 precursor ions with abundances greater than an ion count of 10,000 in the MS survey scan with 30.0s dynamic exclusion. The electrospray voltage applied was 2.0 kV. Automatic gain control (AGC) was used to prevent overfilling of

the ion trap; 50,000 ions were accumulated for generation of MS/MS spectra. For MS scans, the m/z scan range was 350 to 1800. Fixed first mass was set as 100 m/z.

Search of Database

The resulting MS/MS data were processed using Mascot search engine (v.2.3.0). Tandem mass spectra were searched against *Uniprot_zebrafish* database (41,054 sequences). Trypsin/P was specified as cleavage enzyme allowing up to 2 missing cleavages. Mass error was set to 10 ppm for precursor ions and 0.02 Da for fragment ions. Carbamidomethyl on Cys, iTRAQ-8plex (N-term) and iTRAQ-8plex (K) were specified as fixed modification and iTRAQ-8plex (Y), oxidation on Met was specified as variable modifications. False discovery rate (FDR) was adjusted to < 1% and peptide ion score was set ≥ 20 to reduce the probability of false peptide identification.

HR-MAS ^{1}H NMR-based metabolomic analysis

Sample preparation and ^{1}H NMR spectroscopy

Each sample of liver was rinsed in saline D_2O at 4 °C to maintain osmolality and to provide a field-lock, and placed into a 4 mm-diameter zirconium oxide (ZrO2) rotor with a spherical insert and a Kel-F cap. The total preparation time for each sample was less than 5 min. All high resolution magic-angle-spinning (HR-MAS) ^{1}H NMR spectra were recorded on a Bruke Avance 600 NMR spectrometer (Bruker Biospin, Germany) equipped with a triple-field resonance (^{1}H/^{13}C/^{31}P) high-resolution MAS probe, operating at a ^{1}H frequency of 600.13 MHz. Samples of tissue were spun at 5 KHz at the "magic-angle" (54.7°) and maintained at 283 K to minimize temperature-dependent metabolic changes. The one-dimensional Carr-Purcell-Meiboom-Gill (CPMG) spin-echo pulse sequence (recycle delay -90°-(τ-180°-τ)$_n$-acquisition) with a fixed total spin-spin relaxation delay, 2 nτ of 64 ms, was applied to acquire ^{1}H MAS NMR spectra of all samples. Water signals were pre-saturated by weak continuous wave irradiation on water resonance during the recycle delay. Typically, 64 transients were acquired with 32 K data points for each spectrum with a spectral width of 12.012 kHz, and the 90° pulse length was adjusted to approximately 9.5 μs for 90° pulse calibration individually for each sample. For assignment purpose, a series of 2D NMR spectra were acquired for some selected samples, including ^{1}H-^{1}H correlation spectroscopy (COSY), ^{1}H-^{1}H total correlation spectroscopy (TOCSY), ^{1}H J-resolved spectroscopy (JRES), ^{1}H-^{13}C heteronuclear single quantum correlation spectroscopy (HSQC), and ^{1}H-^{13}C heteronuclear multiple bond correlation spectroscopy (HMBC).

Processing of NMR Spectra

NMR spectra were processed by use of MestReNova (version 7.0, Mestrelab Research, Spain) and all free induction decays (FIDs) were multiplied by use of an exponential weighting function with a 0.3-Hz line broadening factor prior to Fourier transformation. Resulting NMR spectra were manually phased and baseline-corrected, then referenced to the internal lactate CH_3 resonance at 1.33 ppm. The spectral region

9.5-0.5 ppm was automatically divided into integral segments of equal width (0.004 ppm) and the regions of 6.08-5.45 ppm and 5.22-4.68 ppm (water) were removed.

Pattern Recognition Analysis and Statistics

For multivariate statistical analyses, after normalization of the spectra to the total integration value for each spectrum data from NMR spectra were imported to SIMCA-P+ (V11.0, Umetrics, Umea, Sweden). Principal component analyses (PCA) were performed by using a unit variance (UV) scaling approach, and the data were visualized in the form of PC score plots, in which each point represented an individual sample. A more sophisticated discriminant technique, partial least squares discriminant analysis (PLS-DA), was further applied to achieve global profile separation between the different treatments through maximizing systematic variance. Qualities of models were evaluated by 6-fold cross-validation parameters: R^2, indicating the total explained variation for the NMR data, and Q^2, indicating the predictability of the model, and an additional validation method, permutation test (permutation number = 200) was also conducted. Finally, the orthogonal projection to latent structure with discriminant analysis (OPLS-DA) method was utilized to identify the differential metabolites responsible for MC-LR exposure on unit variance scaled data. Coefficient plots provide information on spectral regions responsible for classification of samples and the significance of such contribution. Loadings in coefficient plots were calculated back from coefficients incorporating weights of variables contributing to the sample classification in the model. Coefficient plots were generated by use of MATLAB scripts (http://www.mathworks.com) with some in-house modifications and were color-coded with absolute value of coefficients (r). Correlation coefficients ($|r|$) > 0.755, which was determined according to the test for the significance of the Pearson's product-moment correlation coefficient, were considered statistically significant based on the discrimination significance at the level of $p < 0.05$ and degrees of freedom = 5.

Table S1. Quantitative real-time PCR (qRT-PCR) primer sequences for selected genes

Gene name	Abbreviation	Primer Sequence (5'-3')		Accession number	Product length (bp)
		Forward	Reverse		
phosphofructokinase, liver b	pfklb	GGATTTGAGGCGTATGAAGGA	TGATGGTGGCAGGAATGAC	NM_001328389.1	97
pyruvate kinase, liver and RBC	pklr	AACACAGATGCTGGAGAGTATG	CTCTACAGGGAAGTGTCCTTTG	NM_201289.1	139
pyruvate dehydrogenase (lipoamide) alpha 1a	pdha1a	CTGGTTGGACCCTCTCCTATTA	TCAATGTGGCTGGGAGATTTAG	NM_213393.1	112
succinate dehydrogenase complex, subunit A, flavoprotein (Fp)	sdha	CTCTGAGACCGCCATGATTT	GATGACCTGTCCCTTGTAGTTG	AY391458.1	118
NADH dehydrogenase subunit 1	nd1	TTGATGCTCAACCTGATCCC	CCCTATCCAGTACTCGACCTAA	KM207051.1	97
cytochrome c oxidase subunit I	coxI	GACGCCTATGCACTCTGAAATA	GGCGGTAAAGGCTTCTCATAA	AY996924.1	102
ATP synthase 6, mitochondrial	atp6	CCTTATCCTCGTTGCCATACTT	GTTTGTGAATCGTCCAGTCAATC	KT624627.1	115
protein disulfide isomerase family A, member 3	pdia3	GAGTTCTCTCGTGATGGAAAGG	CAGGAACGGGCTCAGATTTA	NM_001199737.1	94
peptidyl-prolyl cis-trans isomerase A-like	ppctia	CACTGACTGTGGAGAACTCAAG	ACCCAGAGCGTTCACATTATC	NM_001327972.1	101
endoplasmic reticulum to nucleus signaling 1, zebrafish homolog of human IRE1	ern1	ATGGGTAAGAAGCAGGATGTG	CAGGGACGAAGATGGACATAAC	NM_001020530.1	108
X-box binding protein 1, alternatively spliced	xbp1-1s	GATCCACTTCGACCACATCTAC	GACGGAATCCTCAGCTTTAACT	AY237651.1	88
eukaryotic translation initiation factor 2-alpha kinase 3, zebrafish homolog of human PERK	eif2ak3	GCCTCAGCAAACCAGAGATT	CTGAAGGAAACAGCCTCCATAC	BC122104.1	109
eukaryotic translation initiation factor 2, subunit 1 alpha a, zebrafish homolog of human eIF2α	eif2s1a	TTGATTGCTCCTCCTCGATATG	GCCTCTCTTCTCTTCGATCTTC	NM_199569.1	117
activating transcription factor 6	atf6	AAACCTCCACCTGTCACTATTC	CATTGACTGAGGCGTCTGAA	NM_001110519.1	102
activating transcription factor 4	atf4	CACACTGAGGTTCCAGTTCTC	TCGCTAATGTTCTGCTCTTCTT	BC067714.1	104
heat shock protein 5, zebrafish homolog of human glucose regulated protein 78	hspa5	GTGAACGAAGCCGAGAGATT	CGATCTGGTTCTTCAGGGAATAG	NM_213058.1	106
heat shock protein 90, beta (grp94)	hsp90b1	AGGCCCTGAAGGAACAAATC	CATGTTTCCAGACCATCCATACT	NM_198210.2	101
DNA-damage-inducible transcript 3, zebrafish homolog of human CHOP	ddit3	CTTCTTGTGGAGAGCGTGAAA	CGGTGGGAGACATTCACTAAAC	NM_001082825.1	97
glyceraldehyde-3-phosphate dehydrogenase	gapdh	AACCGTGTATGTGACCTGATG	TTCAACCAGATGGGAGAATGG	NM_001115114.1	104
18S small subunit ribosomal RNA	18S rRNA	GAGACTCCGGCATGCTAAAT	CAGACCTGTTATTGCTCCATCT	FJ915075.1	108

Table S2 Number of altered proteins in liver of zebrafish exposed to MC-LR.

		1 μg/L MC-LR vs control	10 μg/L MC-LR vs control
up-regulated	annotated/total	9/12	22/44
down-regulated	annotated/total	11/25	17/37
de-regulated	annotated/total	20/37	39/81

Table S3. Differentially expressed proteins (with functional annotation) in liver of zebrafish exposed to MC-LR.

Protein accession	Protein description	MW [Da]	pI	AASC [%]	MP	Score	Fold change[a]		Function category
							1 μg/L	10 μg/L	
Amino acid metabolism									
F1Q6E1	4-hydroxyphenylpyruvate dioxygenase	55878	6.21	48.2	18	1443	2.09±0.25	2.18±0.06*	tyrosine metabolism
Q6TGZ5	4-hydroxyphenylpyruvate dioxygenase	56913	6.33	50.9	19	1402	0.28±0.00**	0.30±0.02**	tyrosine metabolism
F1QHM8	Methylthioribulose-1-phosphate dehydratase	33409	6.1	12.9	2	73	0.98±0.03	0.73±0.03*	methionine metabolism
Q1RLT0	S-adenosylmethionine synthase	53891	6.38	12.8	3	55	1.02±0.02	0.72±0.01**	methionine metabolism
Protein metabolism									
A8E526	Rpl14 protein	23533	10.34	36.7	5	190	1.52±0.15	1.28±0.04*	ribosome biogenesis and assembly; protein biosynthesis
P62084	40S ribosomal protein S7	29842	10.09	20.6	3	221	1.30±0.06	1.35±003*	ribosome biogenesis and assembly; protein biosynthesis
Q6P5L3	60S ribosomal protein L19	33344	11.46	8.7	1	124	1.85±0.40	1.44±0.03*	ribosome biogenesis and assembly; protein biosynthesis
Q6PBV6	H/ACA ribonucleoprotein complex subunit 2-like protein	23655	9	24.7	2	51	1.40±0.09*	1.12±0.07	ribosome biogenesis and assembly; protein biosynthesis
F1Q5S9	Probable signal peptidase complex subunit 2	30634	7.57	8.9	3	89	1.18±0.06	1.35±0.06*	protein processing
Q6NWJ2	Signal peptidase complex subunit 3 homolog (S. cerevisiae)	24556	8.63	19.4	3	100	1.32±0.14	1.45±0.06*	protein processing
Q7T2E1	SEC13 homolog (S. cerevisiae)	41561	5.04	18.8	3	230	1.14±0.11	1.39±0.09*	protein transport
Lipid metabolism									

A3QK15	Acetoacetyl-CoA synthetase	89178	6.15	14.9	8	124	1.61±0.66	0.69±0.03*	Fatty acid metabolism
Q4V8S5	Acbd7 protein	14575	7.85	48.9	2	128	1.95±0.19*	1.48±0.15	atty-acyl-CoA binding
Q58EG2	Erlin-1	46984	6.18	37.1	11	260	1.12±0.01	1.33±0.03*	lipid metabolism
Q6DRN8	Cdipt protein	26678	6.57	13.1	2	36	0.97±0.04	1.30±0.06*	lipid metabolism
Q7T2J4	Alcohol dehydrogenase 8b	51445	7.8	30.9	11	689	0.90±0.16	0.67±0.05*	lipid metabolism
Q9I8L5	Fatty acid-binding protein 10-A, liver basic	18977	8.87	51.6	5	2021	0.99±0.11	0.82±0.02*	Fatty acid transport
O42364	Apolipoprotein Eb	37491	4.88	6.4	1	35	0.89±0.13	0.72±0.01**	lipid transport; lipoprotein metabolism
Mitochondrial energy metabolism									
Q6AZA2	NADH dehydrogenase (Ubiquinone) flavoprotein 1	62421	8.72	16.3	5	165	0.89±0.03	0.69±0.03*	electron transport chain
Q6IQM2	Cytochrome c	16734	9.46	29.8	2	114	0.85±0.10	0.70±0.04*	electron transport chain
Q9MIY7	Cytochrome c oxidase subunit 2	27964	4.6	10.4	2	42	1.21±0.02*	1.05±0.07	electron transport chain
Other metabolism									
A2BHD8	Beta-hexosaminidase	71741	5.77	29.4	12	480	1.22±0.03*	1.38±0.16	beta-N-acetylhexosaminidase activity
F8W5B8	Phosphorylase	116134	6.09	46.8	28	1911	0.79±0.17	0.70±0.03*	glycogen phosphorylase activity
Q0E671	Cytidine monophosphate sialic acid synthetase 1	59775	7.59	6.7	2	103	1.33±0.07*	1.22±0.09	nucleotidyltransferase activity
Q5CZW2	Uridine phosphorylase	30974	5.47	29.6	3	100	0.75±0.08	0.76±0.03*	nucleotide metabolism
Q7ZUN6	Phosphoribosylaminoimidazole carboxylase, phosphoribosylaminoimidazole succinocarboxamide synthetase	57409	6.99	21.9	6	195	1.08±0.17	0.73±0.02**	nucleotide metabolism
Q8UVG6	Cellular retinol-binding protein type II	21443	6.09	16.3	3	39	0.74±0.15	0.54±0.02**	vitamin A metabolism
Chromatin assembly and modification									
E7F4R5	Histone deacetylase 8	178359	5.44	1.7	2	82	0.82±0.18	0.70±0.02*	histone deacetylase activity

G1K2S9	Histone H3	19721	11.27	5.1	1	42	1.34±0.11	1.59±0.12*	chromatin assembly
Q1RLR9	Histone H2A	47695	9.98	7.6	2	58	1.58±0.07*	1.68±0.23	chromatin assembly
Q6NUW5	Acidic leucine-rich nuclear phosphoprotein 32 family member E	32852	3.86	16	3	164	1.38±0.13	1.23±0.04*	H2A.Z chaperone
Signal transduction									
F1QT29	Calcium uniporter protein, mitochondrial	48911	9.15	5.9	2	79	0.82±0.03*	1.00±0.04	calcium uptake into mitochondria
Q1LWV8	Phosphoinositide phospholipase C	173688	5.69	2	2	55	0.82±0.03*	0.82±0.04	signal transducer activity
Q2L6L1	Protein canopy-1	27138	4.97	23.5	3	125	1.57±0.33	1.52±0.08*	fibroblast growth factor receptor signaling pathway
Q803G3	Serine/threonine-protein phosphatase	39760	5.21	28.8	6	186	0.82±0.01*	0.98±0.03	signal transduction
Immune response									
C1IHU8	Intelectin 1	40147	6.3	9.6	2	100	0.64±0.03**	0.58±0.02**	immune response
Q24JW2	Lysozyme	22596	8.79	15.2	2	69	0.39±0.08*	0.39±0.24	immune response
Q6PFU1	CD81 antigen	31180	5.79	12.3	2	47	0.62±0.04*	0.62±0.13	immune response
Q7ZVM6	Cytotoxic granule-associated RNA binding protein 1, like	44791	8.36	12	2	39	1.18±0.18	1.43±0.03*	immune response
Q6PHG2	Hemopexin	63485	6.14	21.5	9	255	0.58±0.11	0.50±0.05*	inflammatory response
Response to stress									
F1QUW4	Hypoxia up-regulated protein 1	142122	4.98	24.7	15	661	1.29±0.25	1.27±0.03*	response to hypoxia
Q90486	Hemoglobin subunit beta-1	19040	7.7	79.7	10	1929	0.62±0.04*	0.84±0.24	response to hypoxia
E9QH31	Aldehyde dehydrogenase	67706	8.82	19.8	8	164	1.21±0.03*	1.22±0.05	oxidoreductase activity
F1QUR3	Protein disulfide-isomerase (Fragment)	67626	6.76	42.5	16	1248	1.30±0.21	1.44±0.10*	protein folding
Q6NYZ0	Dnajb11 protein	49612	5.63	15.3	3	148	1.27±0.23	1.28±0.03**	protein folding
Q6PE26	Calr protein	63340	4.38	35.2	13	491	1.56±0.34	1.47±0.05**	protein folding
Q7ZZA3	Peptidyl-prolyl cis-trans isomerase	26598	7.68	19.8	3	82	1.50±0.11*	1.20±0.10	protein folding
Z4YIA7	Calumenin-A	46617	4.46	27.8	5	199	1.51±0.22	1.48±0.04*	protein folding

Other function									
Q7SXF6	Cysteine-rich with EGF-like domain protein 2	47349	4.6	6.7	2	35	1.40±0.40	1.39±0.03**	calcium ion binding
Q7ZT36	Parvalbumin 3	15248	4.43	50.5	5	100	0.74±0.03*	1.12±0.27	calcium ion binding
E9QB46	Selenium-binding protein 1	62051	5.93	21.6	5	279	1.34±0.09	1.44±0.04*	selenium binding
Q6DGU5	Solute carrier family 25 member 46	48930	8.42	11.4	2	51	0.81±0.01*	0.84±0.01	mitochondrial membrane fission; transport
F1QT89	Reticulon	27018	8.43	16.8	2	66	1.13±0.11	1.24±0.03*	membrane morphogenesis
Q5U3G0	Progesterone receptor membrane component 1	26524	4.75	20.7	3	150	1.35±0.12	1.62±0.07**	progesterone receptor
Q64HD0	Sex hormone binding globulin	50714	5.63	13.9	4	109	0.71±0.02*	0.79±0.08	sex hormone transport
F1QRA6	Tetratricopeptide repeat protein 38	60923	5.78	21.9	8	250	0.93±0.11	0.73±0.02*	unknown
Q8AW82	Novel protein similar to human proliferation-associated 2G4 protein (PA2G4)	57080	8.03	18.4	6	132	1.22±0.02*	1.03±0.03	growth regulation

[a] The fold changes are indicated as compared to the controls. Values >1 indicate up-regulation, and values < 1 indicate down-regulation. Proteins with fold difference > 1.2 or < 0.83 and $p < 0.05$ were considered significantly altered, which are indicated with * ($p < 0.05$) or ** ($p < 0.01$).

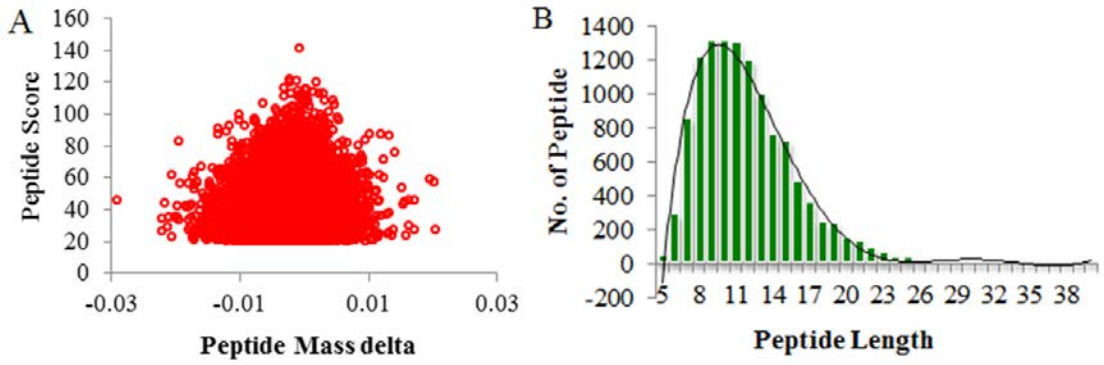

Figure S1. Quality control validation of mass spectrometry data (A) mass error distribution and (B) peptide lengths of peptides identified by iTRAQ.

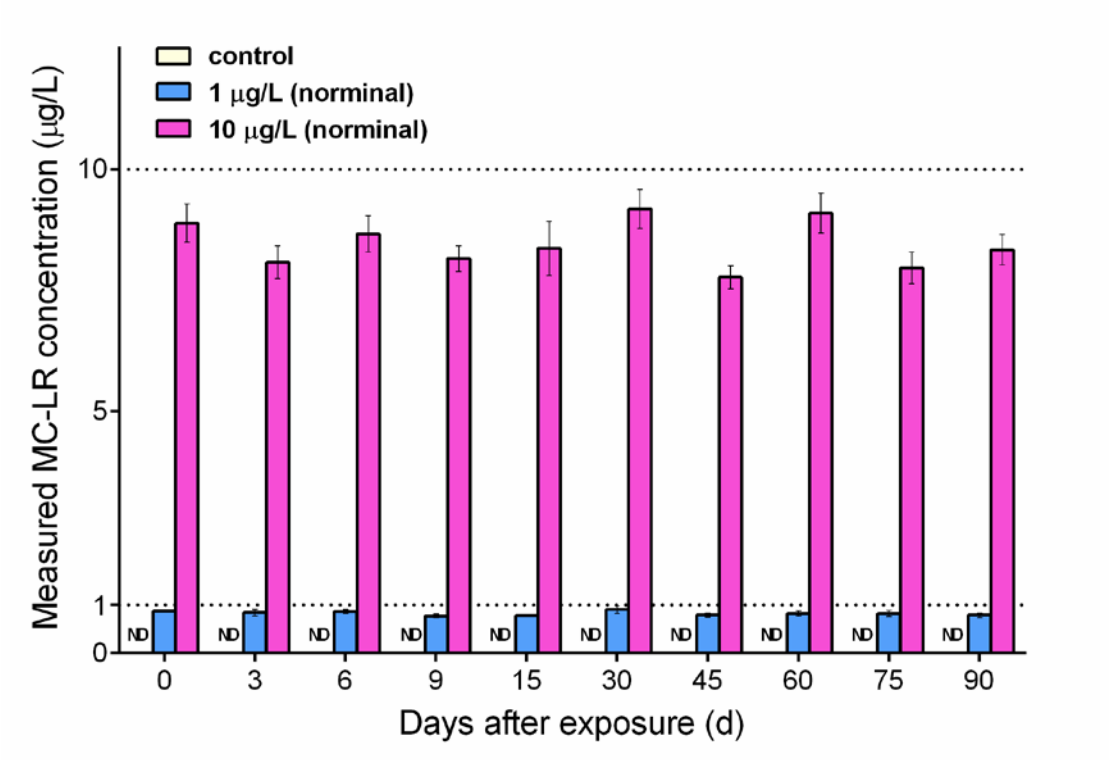

Figure S2. Concentrations of MC-LR measured in water during the 90-day study. Values are presented as the mean ± standard error (SE). ND, indicates not detected, i.e. lower than the minimum detection limit (MDL, 0.1 μg/L).

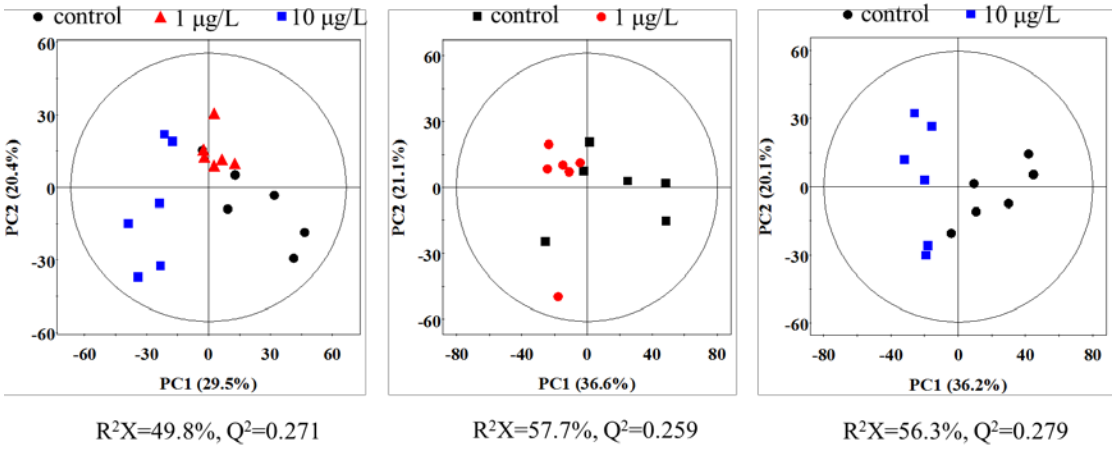

R^2X=49.8%, Q^2=0.271 R^2X=57.7%, Q^2=0.259 R^2X=56.3%, Q^2=0.279

Figure S3. PCA score plots based on ^{1}H HR-MAS CPMG NMR spectra of livers of zebrafish exposed to MC-LR.

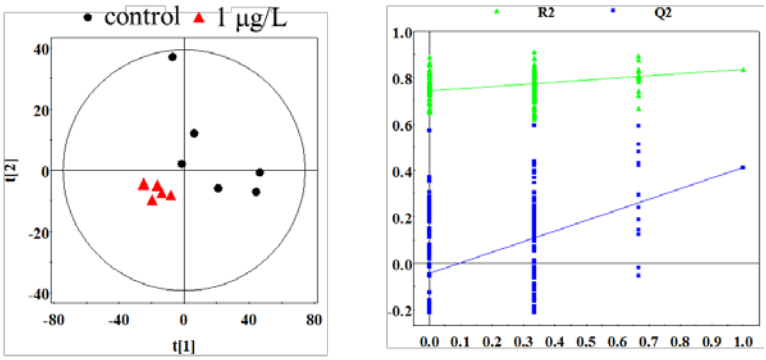

R^2X=45.5%, R^2Y=0.836, Q^2=0.414

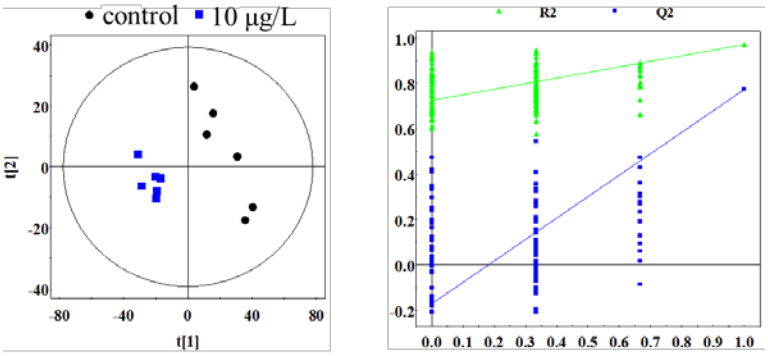

R^2X=46.0%, R^2Y=0.971, Q^2=0.774

Figure S4. PLS-DA score plots (left panel) derived from ^{1}H HR-MAS CPMG NMR spectra of livers of zebrafish exposed to MC-LR and cross validation (right panel) by permutation test (n=200).